

Proton capture cross section of ^7Be and the flux of high energy solar neutrinos

B. W. Filippone*

Argonne National Laboratory, Argonne, Illinois 60439

and Department of Physics, The University of Chicago, Chicago, Illinois 60637

A. J. Elwyn† and C. N. Davids

Argonne National Laboratory, Argonne, Illinois 60439

D. D. Koetke

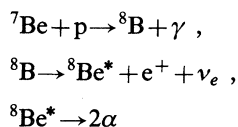
Valparaiso University, Valparaiso, Indiana 46383

(Received 25 July 1983)

The low energy cross section for the $^7\text{Be}(p,\gamma)^8\text{B}$ reaction has been measured by detecting the delayed α particles from the ^8B beta decay. Detailed discussion is presented of the analysis of the radioactive ^7Be target including the use of two independent methods to determine the ^7Be areal density. The direct capture part of the cross section is subtracted from the total cross section to deduce resonance parameters for the 1^+ first excited state in ^8B . The zero-energy astrophysical S factor inferred from the present experiment is compared with previous values. The effect on the ^{37}Cl solar neutrino capture rate, predicted by the standard solar model, is also discussed.

I. INTRODUCTION

For the past 20 years Davis *et al.*¹ have attempted to detect neutrinos originating from nuclear reactions in the solar interior by measuring the capture rate in a ^{37}Cl detector. These neutrinos provide the only direct probe of the conditions at the center of the sun. The agreement between the calculated and measured rates has not been good, differing by factors of 2–10. A key input to the calculations are the rates for the nuclear reactions involved in the proton-proton chain.² The reaction sequence



is expected to terminate the proton-proton chain only once in $\sim 13\,000$ cycles through the chain. It is this sequence, however, which contributes $\sim 75\%$ to the predicted solar neutrino capture rate of 7–8 SNU (Refs. 3 and 4) ($1 \text{ SNU} \equiv 10^{-36} \text{ } \nu \text{ captures/target atom sec}$) in a ^{37}Cl neutrino detector because such a detector is mainly sensitive to the high energy neutrinos from ^8B decay. The measured capture rate is $1.8 \pm 0.3 \text{ SNU}$.¹ This discrepancy represents the so-called solar neutrino problem. To calculate the rate of the $^7\text{Be}(p,\gamma)^8\text{B}$ reaction in the solar interior one needs measured cross sections as low in energy as possible in order to permit accurate extrapolation to the very low energies ($\sim 20 \text{ keV}$) at which most of the reactions occur in the sun.

The low energy cross section for the $^7\text{Be}(p,\gamma)^8\text{B}$ reaction, and the resulting cross section factor,

$$S(E_{c.m.}) = \sigma(E_{c.m.}) E_{c.m.} \exp[(E_G/E_{c.m.})^{1/2}], \quad (1)$$

where

$$E_G = (2\pi\alpha Z_1 Z_2)^2 \mu c^2 / 2 = 13798.8 \text{ keV},$$

(where μ is the reduced mass of the incident channel and α is the fine structure constant) has been measured in five independent experiments since 1960. The pioneering experiment of Kavanagh⁵ measured the cross section to $\pm 40\%$ at proton energies of 0.8 and 1.4 MeV by detecting the high energy positrons from the ^8B decay. Tombrello⁶ used these data to calculate an extrapolated value of $S_{17}(0) = 0.021 \pm 0.008 \text{ keV b}$. Parker⁷ achieved substantial background reduction by detecting the α particles from $^8\text{Be}^*$ breakup following ^8B β^+ decay. This technique has been used in all subsequent $^7\text{Be}(p,\gamma)^8\text{B}$ experiments. The measurements of Parker were made at eight proton energies in the range $E_p = 0.483\text{--}1.952 \text{ MeV}$ with an overall uncertainty of $\pm 10\%$. Using the calculation of Ref. 6, a value of $S_{17}(0) = 0.043 \pm 0.004 \text{ keV b}$ was obtained. These data were later reanalyzed⁸ to give a modified value of $0.035 \pm 0.004 \text{ keV b}$. An extensive series of measurements from $E_p = 0.165$ to 10.0 MeV was reported by Kavanagh *et al.*⁹ and by Kavanagh.¹⁰ The extrapolated zero-energy S factor, again based on the calculation of Ref. 6, was $0.0335 \pm 0.003 \text{ keV b}$. In the experiment of Vaughn *et al.*¹¹ the cross section was determined at 20 proton energies from $E_p = 0.953$ to 3.281 MeV . Two methods of analysis, which depended on the assumed resonance structure in ^8B , yielded $S_{17}(0) = 0.0263 \pm 0.0027$ and $0.0226 \pm 0.0043 \text{ keV b}$. The most recent measurement¹² of the $^7\text{Be}(p,\gamma)^8\text{B}$ reaction was performed at only one energy ($E_p = 360 \text{ keV}$). If this one point is used to normalize the calculation of Ref. 6, the inferred value of $S_{17}(0)$ is

0.045 ± 0.011 keV b.

It is important to note that nearly all of the experiments discussed above^{5,7-11} relied on the value of the $^7\text{Li}(d,p)^8\text{Li}$ cross section at the $E_d = 0.77$ MeV resonance to determine the absolute $^7\text{Be}(p,\gamma)^8\text{B}$ cross section (see Sec. III). The resulting S factors depend linearly on the $^7\text{Li}(d,p)^8\text{Li}$ cross section. The values for this cross section used in the above analyses ranged from 176 to 211 mb; however, two recent measurements of this cross section have obtained 146 ± 13 (Ref. 13) and 148 ± 12 mb.¹⁴

In light of the key role played by the $^7\text{Be}(p,\gamma)^8\text{B}$ reaction in the determination of the ^{37}Cl solar neutrino capture rate, we have measured the cross section down to $E_{c.m.} = 117$ keV ($E_p = 134$ keV) by detecting the β^+ -delayed α particles. Two independent methods were used to determine the absolute value of the cross section, one of which is independent of the $^7\text{Li}(d,p)^8\text{Li}$ reaction. The zero-energy S factor from the present experiment is combined with solar model calculations to determine a new value for the predicted ^{37}Cl solar neutrino capture rate.

II. EXPERIMENTAL PROCEDURE

Proton beams were obtained from the Argonne National Laboratory 4.5 MV dynamitron accelerator, with currents between 4 and 8 μA , limiting the beam power on target to $\lesssim 5$ W. Following magnetic analysis the beam was collimated to produce a beam spot of 3.2 mm on target. For the lower energy points a quadrupole doublet was used to focus the beam. In order to ensure a stable, uniform beam spot, a sawtooth-wave voltage was applied to two orthogonal sets of parallel plates (at incommensurate frequencies) prior to beam collimation. While most of the measurements utilized the H^+ beam, the lowest energy point ($E_{c.m.} = 117$ keV) employed an H_2^+ molecular ion beam. This beam permitted a measurement at a proton energy below the normal energy range of the machine. The energy scale of the dynamitron was determined to $\pm 0.5\%$ from thick target yield curves at resonances in the $^{19}\text{F}(p,\alpha\gamma)^{16}\text{O}$ reaction at proton energies of 224.4, 340.46, and 872.11 keV.

The experimental apparatus, shown schematically in Fig. 1, is essentially the same as that used for the $^7\text{Li}(d,p)^8\text{Li}$ cross section measurement of Ref. 14. The target was mounted on a rotating arm and could be transferred (transfer time ~ 0.3 sec) from the bombardment chamber to the counting chamber by a signal to the stepping motor. A collimated silicon surface barrier detector with 300 mm^2 active area and 23 μm depletion depth was mounted in the counting chamber to detect the β^+ -delayed α particles. The detector was mounted in a "near" geometry configuration of ~ 2 mm target-collimator distance. In this tight geometry the use of a very thin detector is required because of the large background of electrons produced by the 478 keV γ rays from the ^7Be target ($\sim 3 \times 10^8$ γ/sec). To help reduce this background the detector mount and collimator were made from low Z material and the detector itself was of the ring-mount-type in which the thin silicon crystal is supported only by a ceramic ring. The system was pumped

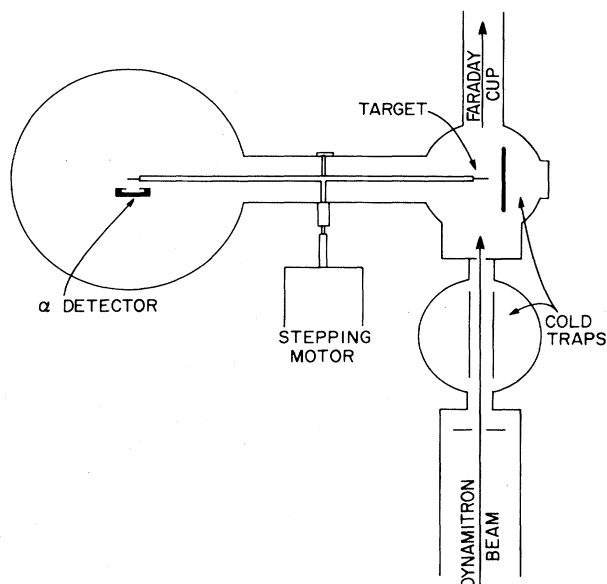


FIG. 1. Schematic diagram of the target apparatus.

by a turbomolecular pump in the counting chamber and large area liquid nitrogen-cooled surfaces in the bombardment chamber to a pressure of $\lesssim 5 \times 10^{-7}$ Torr. The use of an oil-free pump and cold surfaces near the beam limited the proton energy loss due to carbon buildup on the target to $\lesssim 3$ keV throughout the course of the experiment.

The solid angle of the detector in the "near" geometry was measured to be $(23.1 \pm 1.5)\%$ of 4π sr. This was determined by comparing the yield of α particles from the $^7\text{Li}(d,p)^8\text{Li} \rightarrow ^8\text{Be}^* \rightarrow 2\alpha$ reaction in the "near" geometry to that in a "far" geometry in which the target-collimator distance was 22.2 mm. An average value from the measured geometry and a calibrated ^{241}Am source then gave the solid angle in the "far" geometry. The current integration of the beam and the control of the timing cycle are described in Ref. 14. The intervals of the timing cycle were the following: $t_1 \equiv$ beam on target = 1.50 sec; $t_2 \equiv$ transfer to counting = 0.52 sec; $t_3 \equiv$ counting = 1.50 sec; $t_4 \equiv$ transfer to bombardment = 0.52 sec.

The ^7Be used in the preparation of the target was produced via the $^7\text{Li}(p,n)^7\text{Be}$ reaction at the Argonne dynamitron. A proton beam of 3.6 MeV bombarded a chemically purified and isotopically enriched 25 mg/cm^2 ^7Li metal target, produced by vacuum evaporation onto a water-cooled Cu backing. Approximately 120 mCi of ^7Be were produced from the 5000 $\mu\text{A h}$ bombardment. After bombardment ^7Be was chemically separated and purified by repeated solvent extraction and ion exchange. It was then deposited onto a 0.25 mm thick Pt disk by the molecular plating method,¹⁵ which involves high voltage electro-deposition from an organic solution. The target was then flamed red-hot in air for several minutes to convert the ^7Be to beryllium oxide and to remove any volatile contaminants. The final target consisted of ~ 80 mCi of ^7Be (~ 0.23 μg) and ~ 7 μg of solids. Details of the target

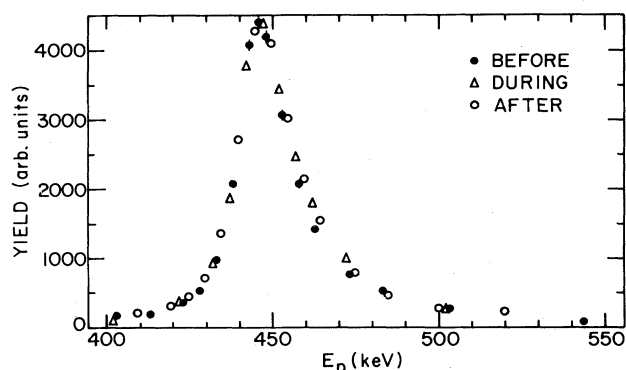


FIG. 2. ${}^7\text{Li}(p,\gamma){}^8\text{Be}$ excitation function for the ${}^7\text{Be}$ target. These data represent three separate measurements performed before, during, and after the ${}^7\text{Be}(p,\gamma){}^8\text{B}$ experiment. The relative uncertainties are approximately the size of the points.

preparation will be published elsewhere.¹⁶

The energy thickness of the target and the energy loss due to carbon buildup on the target were measured in studies of the shape of the resonance curve for the ${}^7\text{Li}(p,\gamma){}^8\text{Be}$ reaction at the 441.4 keV resonance ($\Gamma_{\text{lab}} = 12.2 \pm 0.5$ keV). For this analysis it was assumed that the lithium and beryllium reside at the same location in the target since essentially all of the ${}^7\text{Li}$ in the target is due to ${}^7\text{Be}$ decay (see below). This assumption was verified in a separate experiment whose aim was to investigate resonances in the ${}^7\text{Be}(\alpha,\gamma){}^{11}\text{C}$ reaction¹⁷ using the same target. The energy loss of the α beam agreed well (when the relative proton and α stopping powers were taken into account) with that obtained from the ${}^7\text{Li}(p,\gamma){}^8\text{Be}$ data (within the $\pm 15\%$ uncertainty in the energy loss). Resonance curves for the ${}^7\text{Li}(p,\gamma){}^8\text{Be}$ reaction are shown in Fig. 2. These data were taken with a 25.4×25.4 cm NaI(Tl) crystal at 90° to the beam, and were corrected for a continuous buildup of carbon (to a maximum of 3 keV) as well as for the increasing amount of ${}^7\text{Li}$ from the decay of ${}^7\text{Be}$.

The most difficult quantity to determine in the experiment is the ${}^7\text{Be}$ areal density. In the past, most workers measured the yield of the ${}^7\text{Li}(d,p){}^8\text{Li}$ reaction at the 0.77-MeV resonance, and, with the known resonant cross section, determined the buildup of ${}^7\text{Li}$ from the ${}^7\text{Be}$ decay in the target. With this value, and by use of the relation

$$N_{{}^7\text{Li}}(t) = N_{{}^7\text{Be}}(0)(1 - e^{-\lambda t}) + N_{{}^7\text{Li}}(0), \quad (2)$$

where $\lambda (= 1.505 \times 10^{-7} \text{ sec}^{-1})$ is the ${}^7\text{Be}$ decay constant, the ${}^7\text{Be}$ areal density, or, if the same detector geometry is used for both the ${}^7\text{Li}(d,p)$ and ${}^7\text{Be}(p,\gamma)$ reactions, the product of ${}^7\text{Be}$ areal density and detector solid angle, can be obtained. One previous experiment¹² made use of the total γ -ray activity of the target and the area of the target spot to determine the ${}^7\text{Be}$ areal density; however, none of the previous experiments utilized both methods. Because of inconsistencies in the measured value of the ${}^7\text{Li}(d,p){}^8\text{Li}$ cross section¹⁸ both methods were employed in the present experiment.

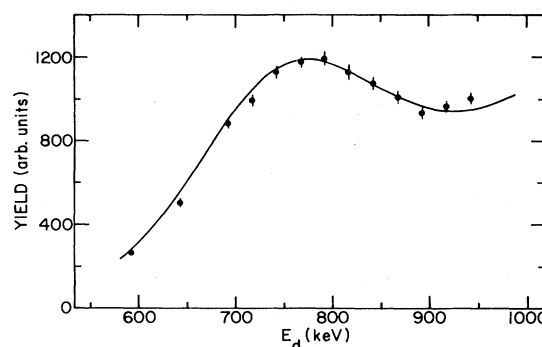


FIG. 3. ${}^7\text{Li}(d,p){}^8\text{Li}$ excitation function for the ${}^7\text{Be}$ target. The solid curve is an excitation function for the ${}^7\text{Li}(d,p){}^8\text{Li}$ reaction for a thin ${}^7\text{LiF}$ target normalized to the data.

An excitation curve for the ${}^7\text{Li}(d,p){}^8\text{Li}$ reaction from deuteron bombardment of the ${}^7\text{Be}$ target is shown in Fig. 3. This measurement utilized the same apparatus (Fig. 1) as was used for the ${}^7\text{Be}(p,\gamma)$ reaction. The molecular ion beam D_3^+ was used because a time- and source-dependent contamination of the mass 2 beam (D^+) with molecular hydrogen (H_2^+) was observed in backscattering experiments from a thin gold foil. The yield of α particles at the peak of the 0.77 MeV resonance as a function of $(1 - e^{-\lambda t})$ is displayed in Fig. 4. The measurements were made over a period of five weeks during which time the ${}^7\text{Be}(p,\gamma){}^8\text{B}$ experiment was performed. A linear least-squares fit to these data shows that there was essentially no ${}^7\text{Li}$ in the target on the final day of chemical separation and purification. In fact, the intercept corresponded, within several hours, to the time of the final electroplating and flaming of the target. The slope of the curve [see Eq. (2)] yields a product of ${}^7\text{Be}$ areal density and detector solid angle fraction ($\Omega/4\pi$) of $(2.24 \pm 0.15) \times 10^{16}/\text{cm}^2$. This was determined by use of a (d,p) cross section (σ_{dp}) of 157 ± 10 mb (see Sec. IV) and the expression for the cross section described in Sec. III.

For the second method used to determine the ${}^7\text{Be}$ areal

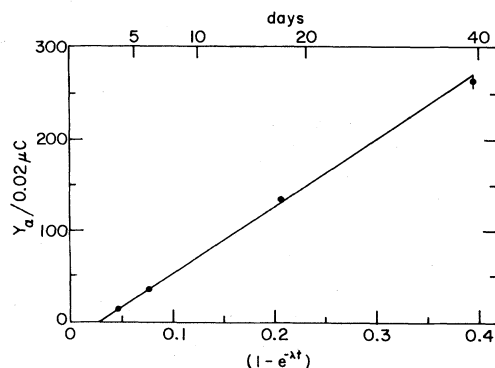


FIG. 4. The buildup of ${}^7\text{Li}$ in the ${}^7\text{Be}$ target as monitored by the increasing yield of α particles from the sequence ${}^7\text{Li}(d,p){}^8\text{Li} \rightarrow {}^8\text{Be}^* \rightarrow 2\alpha$ as a function of $(1 - e^{-\lambda t})$, where λ is the ${}^7\text{Be}$ decay constant. The solid line is a linear least-squares fit to the data.

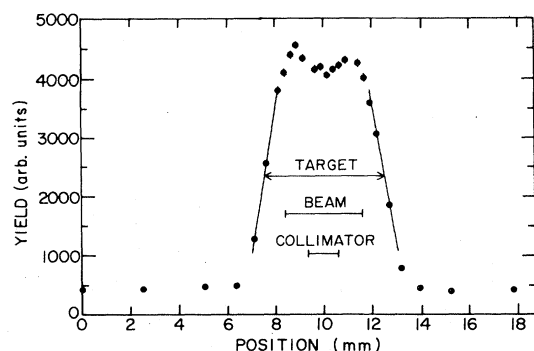


FIG. 5. The yield of 478 keV γ rays from the ^7Be target as a function of position for the 1.3 mm Pb collimator. Also shown are the diameters of the target, beam spot, and collimator.

density, the total number of ^7Be nuclei in the target was found by measuring the yield of 478 keV γ rays in a Ge(Li) detector whose absolute full energy peak efficiency was determined using calibrated γ -ray sources of ^{54}Mn , ^{133}Ba , and ^{137}Cs . After correcting for decay and using a ^7Be branching ratio (to the 478 keV state in ^7Li) of $(10.35 \pm 0.10)\%$, the average of two measurements gave an initial total activity of 81.2 ± 6.0 mCi. The area of the target was determined by scanning the γ -ray activity of the target spot with a NaI(Tl) detector and two 10 cm thick Pb collimators with 0.5 and 1.3 mm diam apertures. Figure 5 shows a γ -ray scan for the 1.3 mm diam collimator. The nonuniformities in the target were on the order of 5–10%, but when averaged over the beam spot they amounted to $\leq 5\%$ uncertainty in the areal density. From a total of six scans with different target orientations the diameter of the target spot was found to be 4.95 ± 0.15 mm by calculating the shape of the curve expected from a circular aperture intersecting a circular target spot. The correction for the finite size of the apertures in the present experiment differed from the FWHM by less than 0.05 mm. The product of ^7Be areal density and solid angle fraction which results from the separate measurements of ^7Be activity, target diameter, and solid angle is $(2.40 \pm 0.27) \times 10^{16}/\text{cm}^2$. This is in excellent agreement with the value extracted from the $^7\text{Li}(d,p)^8\text{Li}$ yield curve in Fig. 4, as discussed above.

III. RESULTS AND ANALYSIS

The spectra of β^+ -delayed α particles observed from the $^7\text{Be}(p,\gamma)^8\text{B}$ reaction at $E_{\text{c.m.}} = 632$ and 117 keV are shown in Fig. 6. These energies correspond to the highest and lowest measured cross sections. Also shown in this figure is a background spectrum taken with the beam off and the ^7Be target in front of the α detector. The equivalent running times for the three spectra are 2, 30, and 66 h, respectively. The effect of the high flux of γ rays that come from the decay of ^7Be can be seen to extend out to ~ 1.0 MeV in the background spectrum. Most of this low energy background was biased out of the spectra to reduce dead times to $\ll 1\%$. The events in the

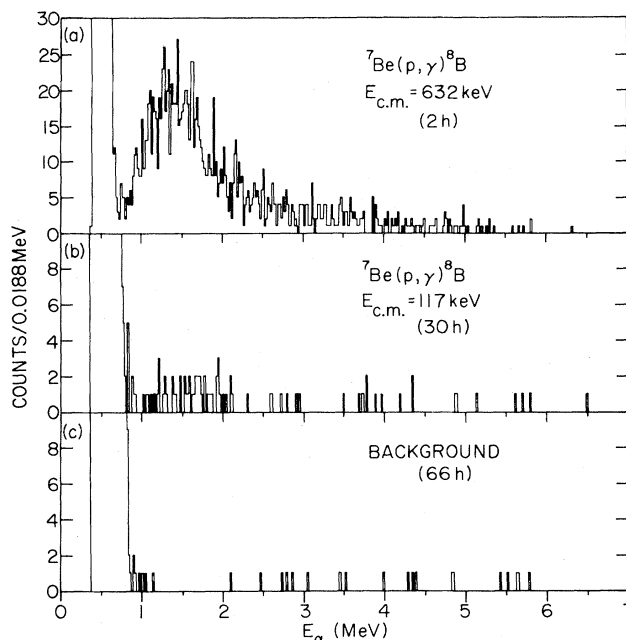


FIG. 6. (a) and (b) Delayed α -particle spectra for the reaction sequence $^7\text{Be}(p,\gamma)^8\text{B} \rightarrow ^8\text{Be}^* \rightarrow 2\alpha$, and (c) a background spectrum.

background spectrum at higher energies are primarily due to natural radioactivity in the detector, mount, and chamber. The integrated α particle yields were obtained from the spectra by accepting all α particles above an energy cut of 0.95 MeV. Detailed studies of the low energy portion of the spectrum of delayed α particles from ^8B and ^8Li decay were performed, and indicated that the data were fit very well by a Gaussian from the peak in the spectrum down to zero energy. From such a Gaussian extrapolation it was found that the energy cut of $E_\alpha > 0.95$ MeV should include $92 \pm 4\%$ of the total yield of α particles at $E_{\text{c.m.}} = 632$ keV. Analysis of the spectra at other energies indicated that the spectra were slightly shifted in energy because the α particles originate from different depths in the target due to the different recoil energy of the ^8B . Reaction kinematics and standard range and energy loss tables²⁰ were used to calculate this effect. These calculations suggested that at the highest and lowest energies in the experiment the $E_\alpha > 0.95$ MeV cut should include $89 \pm 4\%$ and $95 \pm 4\%$ of the total yield, and the data were corrected for this effect.

The background due to natural α emitters and the ^7Be γ rays was measured to be 0.42 ± 0.09 counts/1000 cycles at channels above the 0.95 MeV energy cut, where a cycle is one complete revolution of the target arm. This background amounted to $\leq 2\%$ of the integrated α particle yield for all but the two lowest energy points, where it was 10–15% of the yield. An additional source of background in the experiment is due to possible deuteron contamination of the proton beam. This can be a problem because the (d,p) reaction on the ^7Li in the target produces delayed α particles with a cross section 10^2 – 10^5 times

that for the ${}^7\text{Be}(p,\gamma){}^8\text{B}$ reaction. This background was measured by bombarding thick ${}^7\text{LiF}$ targets with the H^+ and H_2^+ beams. For the H^+ beam the deuteron contamination was found to be $<1 \times 10^{-8}$ at the 90% confidence level. Using the low energy ${}^7\text{Li}(d,p){}^8\text{Li}$ cross section measurements of Ref. 21 this amounts to $<0.5\%$ of the integrated α particle yield for all proton energies, and was neglected. While deuterons are not, in fact, expected in an H^+ beam because of the difference in magnetic rigidity except via rare, complex multiple scattering trajectories, this is not true for the H_2^+ beam, which has the same rigidity as a ${}^2\text{H}^+$ beam. Thus, one would expect the H_2^+ beam to be contaminated by at least the natural abundance of deuterium (on the assumption of equal production of the monatomic and diatomic beams expected to be approximately valid for the ion source used in the experiment). Because of this, the H_2^+ beam could only be used at the lowest proton energy, $E_{\text{H}_2^+} = 0.3$ MeV. This energy is only ~ 50 keV above the (d,p) reaction threshold and the cross section is very small. The background due to contamination of the H_2^+ beam was measured to be only 2% of the integrated α particle yield at $E_{\text{H}_2^+} = 0.3$ MeV, and was consistent with that expected from the natural abundance of deuterium.

The total cross section for the ${}^7\text{Be}(p,\gamma){}^8\text{B}$ reaction was calculated from the formula

$$\sigma(\bar{E}_p) = \frac{Y_\alpha(E_i)\beta({}^8\text{B})}{2N_p N_{7\text{Be}}(t)(\Omega/4\pi)}, \quad (3)$$

where \bar{E}_p is the average energy of the beam in the target (see discussion below), $Y_\alpha(E_i)$ is the background subtracted α particle yield at incident energy E_i , N_p is the total number of incident protons, $N_{7\text{Be}}(t) = N_{7\text{Be}}(0)\exp(-\lambda_{7\text{Be}} t)$ is the number of ${}^7\text{Be}$ nuclei/cm² in the target at time t after chemical separation, and $\Omega/4\pi$ is the solid angle fraction of the α detector. The factor of 2 in the denominator accounts for the two α particles produced in each reaction. The remaining factor is defined as

$$\beta({}^8\text{B}) = \frac{\lambda t_1 \{1 - \exp[-\lambda(t_1 + t_2 + t_3 + t_4)]\}}{(1 - e^{-\lambda t_1})[e^{-\lambda t_2} - e^{-\lambda(t_2 + t_3)}]}, \quad (4)$$

where λ is the ${}^8\text{B}$ decay constant and t_i are the time intervals of the timing cycle described in Sec. III. This factor accounts for ${}^8\text{B}$ decay during bombardment, transfer, and counting, as well as ${}^8\text{B}$ buildup from previous cycles. A half-life²² of 769 ± 4 msec was assumed for ${}^8\text{B}$, which gives $\beta({}^8\text{B}) = 3.829 \pm 0.013$. Equations (3) and (4) were also used to determine the ${}^7\text{Be}$ areal density-solid angle product from the known ${}^7\text{Li}(d,p){}^8\text{Li}$ cross section as discussed in Sec. II. For this determination a ${}^8\text{Li}$ half-life²² of 842 ± 6 msec was assumed, giving $\beta({}^8\text{Li}) = 3.632 \pm 0.014$.

Because of the strong energy dependence in Eq. (1), the effective or average energy of the beam must be known in order to determine the S factor. This energy (\bar{E}_p) is defined as the energy at which the cross section, evaluated at this energy, equals the cross section averaged over the target thickness; that is,

$$\sigma(\bar{E}_p) = \frac{\int_{E_i - \Delta E}^{E_i} \sigma(E') \left[\frac{dE}{dx}(E') \right]^{-1} dE'}{\int_{E_i - \Delta E}^{E_i} \left[\frac{dE}{dx}(E') \right]^{-1} dE'}, \quad (5)$$

where E_i is the incident beam energy corrected for energy loss in the front carbon layer, ΔE is the energy loss in the target, and $(dE/dx)(E')$ is the energy dependent stopping power. To solve this equation the energy dependence of the cross section must be known. For most of the energy range of the experiment the energy dependence of the cross section was taken from Eq. (1) with a constant S factor. Near the $E_p = 0.73$ MeV resonance in the ${}^7\text{Be}(p,\gamma){}^8\text{B}$ reaction (corresponding to the first excited state in ${}^8\text{B}$), a Breit-Wigner term was included in the energy dependence.

The energy loss of the beam in the target was measured to be 15 ± 2 keV at the 441.4 keV resonance in the ${}^7\text{Li}(p,\gamma){}^8\text{Be}$ reaction. When this energy loss is combined with the measured mass of material and the area of the target (see Sec. II) an approximate stopping power at $E_p \approx 440$ keV of 0.4 ± 0.1 keV/ $\mu\text{g cm}^2$ was determined. This value implies that the average atomic number of the material in the target \bar{Z} is <20 . This is consistent with a composition which, aside from the ${}^7\text{Be}$ and oxygen, likely includes light metal oxides, nitrides, nitrates, etc., as well as carbon, all of which could be present as possible contaminants. It is not necessary, however, to know the exact chemical composition of the target for two reasons. First, the energy loss is measured at one energy (441 keV), and second, for $\bar{Z} < 20$ the energy dependence of the stopping power (taken from the global fits of Andersen and Ziegler²³) varies by $\leq 15\%$ in the energy range of the present experiment. It should be noted that a change of 20% in the stopping power gives a change of only 2.4 keV in $E_{\text{c.m.}}$ even at the lowest energy. Therefore, by choosing some element or composition with $\bar{Z} < 20$ (${}^7\text{BeO}$ was used) to characterize the energy dependence of the stopping power, an effective thickness τ can be derived from the known energy loss at 441 keV:

$$\tau = \int_{E_i - \Delta E}^{E_i} \left[\frac{dE}{dx}(E') \right]^{-1} dE', \quad (6)$$

where in this case $E_i = 441$ keV and $\Delta E = 15 \pm 2$ keV. This value for τ can then be used to determine the energy loss ΔE at any given energy E_i by solving the above equation by successive approximation. Once the energy loss at bombarding energy E_i is known, Eq. (5) can be used to calculate the average energy. The results of such calculation indicated that in all cases the average energy deviated from the formula $\bar{E}_p = E_i - \Delta E/2$ by $<1\%$. The good agreement with this formula results because, for the small energy losses involved (the maximum was 25 keV at $E_i = 146$ keV), the stopping power changes by $\sim 5\%$ and the cross section is nearly linear with energy.

As mentioned earlier, the lowest energy point ($\bar{E}_p = 134$ keV) was obtained with an H_2^+ molecular ion beam. As the molecule enters the target the electron is stripped off and the two protons move apart under their mutual elec-

trostatic repulsion—the so-called Coulomb explosion. The net effect of this explosion is to give an overall energy spread to the beam which is symmetric about the beam energy. Simple kinematic considerations, in addition to experimental measurements,²⁴ indicate that the energy distribution is a semicircle centered at the beam energy and that the radius of this semicircle (the maximum energy deviation) is proportional to the square root of the incident beam energy. Calculations of the average energy were performed with such an energy spread by integrating Eq. (5) over all possible energies from the distribution. Even if the energy spread were 4–5 times that which would be expected on the basis of the above discussion (the expected spread is $\Delta E = \pm 2$ keV), because this spread is symmetric about the beam energy, the calculated average energies would differ by $\ll 1\%$ from those calculated without inclusion of the Coulomb explosion.

The center of mass energy has been obtained from the average energy with the expression $E_{c.m.} = 0.87444 \bar{E}_p$. The uncertainty attached to $E_{c.m.}$ was ± 3 keV or 0.5%, whichever was larger. This includes uncertainties in the energy calibration, the extrapolated stopping powers, the extracted energy loss from the ${}^7\text{Li}(p,\gamma){}^8\text{Be}$ resonance, as well as uncertainties in the energy lost in the carbon build-up on the target. The above error in $E_{c.m.}$ amounts to an additional uncertainty in the S factors of 11% and 5% at the two lowest energy points, and only 3% or less at all other energies.

The cross section and derived S factor for the ${}^7\text{Be}(p,\gamma){}^8\text{B}$ reaction as a function of $E_{c.m.}$ are displayed in Figs. 7 and 8. The error bars correspond to relative errors due to counting statistics. Also shown is a least-squares best-fit normalization of the calculation of Tombrello⁶ to

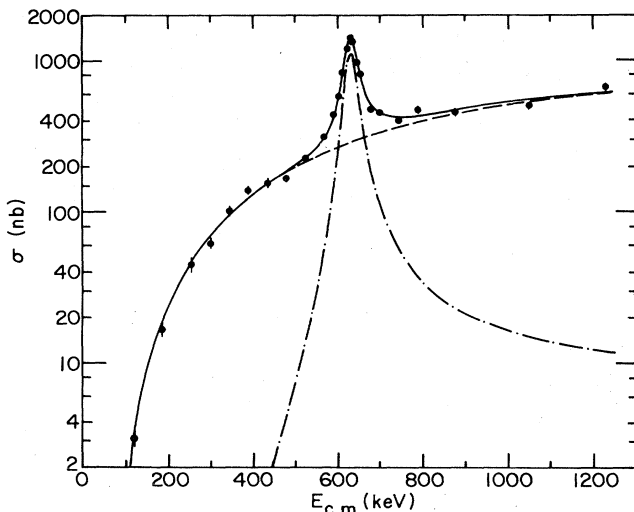


FIG. 7. Total cross section for the ${}^7\text{Be}(p,\gamma){}^8\text{B}$ reaction as a function of the center of mass energy. The dashed curve is the nonresonant direct capture part of the cross section, the dashed-dot curve is the resonant cross section using the parameters discussed in the text, and the solid curve is the sum of the two. If not shown, the error bars (statistical only) are smaller than the data points.

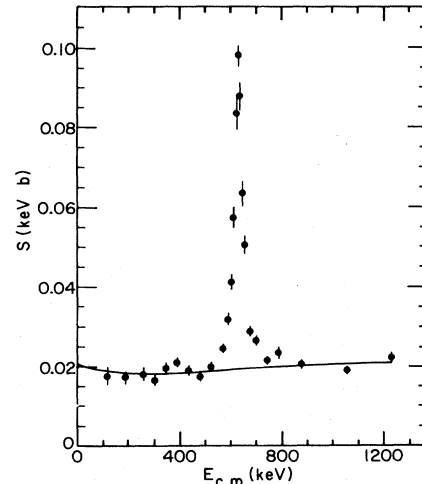


FIG. 8. ${}^7\text{Be}(p,\gamma){}^8\text{B}$ S factor versus center of mass energy. The solid curve is a least-squares normalization of the calculation of Ref. 6 to the off-resonance data.

the off-resonance data. In Sec. IV we describe the calculation of the zero-energy S factor $S_{17}(0)$ from these data and note the effect on the expected ${}^{37}\text{Cl}$ solar neutrino capture rate.

IV. DISCUSSION

The cross section data display a prominent resonance at $E_{c.m.} = 0.63$ MeV atop the direct capture part of the cross section. This resonance corresponds to the 0.77 MeV first excited state in ${}^8\text{B}$. By subtracting the nonresonant part from the total cross section, the resonant cross section can be used to obtain the resonance parameters. A least-squares normalization of the calculation of Tombrello⁶ to the data for $E_{c.m.} < 400$ keV (where the resonance should give little contribution) yields the nonresonant part of the cross section. The resonant cross section can then be fit to a resonance curve of the single-level Breit-Wigner form, including energy-dependent widths determined by the penetrability and γ ray multipolarity. Such a fit yields a center of mass resonance energy of 632 ± 10 keV, a total width (assuming $\Gamma_p \gg \Gamma_\gamma$) of $\Gamma_{c.m.} = 37 \pm 5$ keV, and a peak resonant cross section of 1180 ± 120 nb. With these values the radiative width of the resonance is found to be $\Gamma_\gamma = 0.025 \pm 0.004$ eV. This is in fair agreement with a number of shell model calculations which predict values of Γ_γ from 0.019 to 0.021 eV.²⁵

As discussed in Sec. I, most previous workers have determined $S_{17}(0)$ by a least-squares normalization of the calculation of Tombrello⁶ to experimental cross sections. Such a normalization to the data from this experiment gives a value of $S_{17} = 0.0217 \pm 0.0025$ keV b, where the error includes uncertainties in $E_{c.m.}$, the ${}^7\text{Be}$ areal density, the solid angle, the fraction of α particle yield above the energy cut, as well as in the normalization procedure. The data used for this normalization were in the range $E_{c.m.} < 525$ keV and $E_{c.m.} > 850$ keV. That this range is effectively outside the resonance region was checked by

determining the resonant contribution to the cross section for these energies from the resonant parameters discussed above. The contributions were $\lesssim 5\%$. It should be noted that when the recent calculation of S_{17} by Barker²⁶ is normalized to the data, consistently lower (by 10–15%) values of $S_{17}(0)$ are obtained because of a somewhat different energy dependence in S_{17} .

Before we can compare our results with previous experiments, it is necessary to discuss our adopted value for σ_{dp} of 157 ± 10 mb. The experimental values for σ_{dp} are not in good agreement (see Fig. 6 in Ref. 14). A weighted average of the modern σ_{dp} measurements gives a chi-squared per degree of freedom (χ^2_ν) for the data set of 3.2. These experimental values include one measurement¹⁹ with an unjustifiably small uncertainty and another⁷ which lies 2.8 standard deviations above the weighted mean. If the uncertainty in Ref. 19 is doubled and the measurement of Ref. 7 is deleted from the data set, the weighted mean becomes 157 mb with $\chi^2_\nu = 1.1$. We have therefore adopted a value of $\bar{\sigma}_{dp} = 157 \pm 10$ mb where an overall systematic uncertainty has been added. This value is not very different from the average of $\bar{\sigma}_{dp} = 166 \pm 12$ mb (1σ) adopted in Ref. 4.

A comparison of the previous ${}^7\text{Be}(p,\gamma){}^8\text{B}$ measurements with the present experiment is shown in Fig. 9. Where appropriate, a ${}^7\text{Li}(d,p){}^8\text{Li}$ cross section of 157 mb has been assumed. Aside from the measurement of Ref. 12, where the cross section was measured at a single energy with $\pm 25\%$ uncertainty, the agreement between the experiments is fairly good. A weighted average of all the data gives $S_{17}(0) = 0.0238 \pm 0.0023$ keV b. The effect of this new average value for $S_{17}(0)$ on the predicted capture rate in the ${}^{37}\text{Cl}$ solar neutrino experiment can be calculated using the solar model code of Ref. 3. Using this value for $S_{17}(0)$ the predicted capture rate is 5.6 SNU, $\sim 20\%$ lower than the value of 7.0 SNU determined in Ref. 3 which used a value for $S_{17}(0)$ of 0.032 keV b. In order to obtain a best estimate value for the ${}^{37}\text{Cl}$ capture rate, one should also include a new measurement²⁷ of S_{34} —the ${}^3\text{He}(\alpha, \gamma){}^7\text{Be}$ S factor—in the analysis. If this is done for the calculation of Ref. 3 the predicted rate is 5.9 SNU. A similar modification of the calculation of Ref. 4 gives 6.5 SNU using the present average value for $S_{17}(0)$, and 6.9

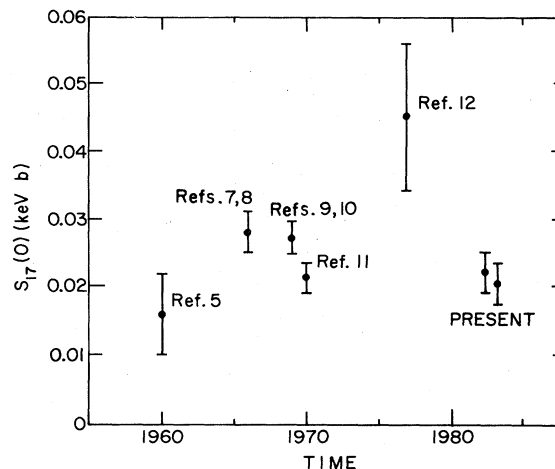


FIG. 9. Summary of the inferred zero-energy S factors from the measurements of the ${}^7\text{Be}(p,\gamma){}^8\text{B}$ reaction. The two values for the present measurement are for the two independent methods used to determine the ${}^7\text{Be}$ areal density.

SNU when the new value²⁷ of $S_{34}(0)$ is included. Here, the dependence of capture rate on input parameters given in Ref. 28 has been used. It is important that continued studies of the nuclear reactions of the proton-proton chain be undertaken in order to eliminate nuclear physics uncertainties as a possible source of the remaining disagreement between theory and experiment.

ACKNOWLEDGMENTS

We thank R. Evans, M. Finn, W. Ray, Jr., and the dynamitron staff for assistance with the experiment. The efforts of M. Wahlgren towards the preparation of the radioactive target are greatly appreciated. We would also like to acknowledge helpful discussions with J. Schiffer, R. Armani, and E. Kanter. This work was supported by the U. S. Department of Energy under Contract W-31-109-Eng-38.

*Present address: Kellogg Laboratory, California Institute of Technology, Pasadena, CA 91106.

¹R. Davis, Jr., in *Proceedings of the Informal Conference on Status and Future of Solar Neutrino Research*, edited by G. Friedlander, BNL Report BNL 50879, 1978, Vol. 1, p. 1; R. Davis, Jr., B. T. Cleveland, and J. K. Rowley, in *Science Underground*, Proceedings of the Workshop on Science Underground, Los Alamos, 1982, edited by M. M. Nieto *et al.*, AIP Conf. Proc. No. 96 (AIP, New York, 1983).

²D. D. Clayton, in *Principles of Stellar Evolution and Nucleosynthesis* (McGraw-Hill, New York, 1968).

³B. W. Filippone and D. N. Schramm, *Astrophys. J.* **253**, 393 (1982).

⁴J. N. Bahcall, W. F. Huebner, S. H. Lubow, P. D. Parker, and R. K. Ulrich, *Rev. Mod. Phys.* **54**, 767 (1982).

⁵R. W. Kavanagh, *Nucl. Phys.* **15**, 411 (1960).

⁶T. A. Tombrello, *Nucl. Phys.* **71**, 459 (1965).

⁷P. D. Parker, *Phys. Rev.* **150**, 851 (1966).

⁸P. D. Parker, *Astrophys. J.* **153**, L85 (1968).

⁹R. W. Kavanagh, T. A. Tombrello, J. M. Mosher, and D. R. Goosman, *Bull. Am. Phys. Soc.* **14**, 1209 (1969).

¹⁰R. W. Kavanagh, in *Cosmology, Fusion and Other Matters*, edited by F. Reines (Colorado University Press, Boulder, 1972), p. 169.

¹¹F. J. Vaughn, R. A. Chalmers, D. Kohler, and L. F. Chase, Jr., *Phys. Rev. C* **2**, 1657 (1970).

¹²C. Wiezorek, H. Kräwinkel, R. Santo, and L. Wallek, *Z. Phys. A* **282**, 121 (1977).

¹³A. J. Elwyn, R. E. Holland, C. N. Davids, and W. Ray, Jr., *Phys. Rev. C* **25**, 2168 (1982).

¹⁴B. W. Filippone, A. J. Elwyn, W. Ray, Jr., and D. D. Koetke, *Phys. Rev. C* **25**, 2174 (1982).

- ¹⁵D. C. Aumann and G. Müllen, Nucl. Instrum. Methods 115, 75 (1974), and references therein.
- ¹⁶B. W. Filippone and M. Wahlgren (unpublished).
- ¹⁷G. Hardie, A. J. Elwyn, B. W. Filippone, R. E. Segel, and M. Wiescher (unpublished).
- ¹⁸See Ref. 14 for a complete discussion of experimental values.
- ¹⁹A. E. Schilling, N. F. Mangelson, K. L. Nielson, D. R. Dixon, M. W. Hill, G. L. Jensen, and V. C. Rogers, Nucl. Phys. A263, 289 (1976).
- ²⁰L. C. Northcliffe and R. F. Schilling, Nucl. Data Tables 7, 233 (1970).
- ²¹C. R. McClenahan and R. E. Segel, Phys. Rev. C 11, 370 (1975).
- ²²F. Ajzenberg-Selove, Nucl. Phys. A320, 1 (1979).
- ²³H. H. Andersen and J. F. Ziegler, *The Stopping and Ranges of Ions in Matter* (Pergamon, New York, 1977).
- ²⁴D. S. Gemmell, Chem. Rev. 80, 301 (1980).
- ²⁵See Ref. 26 for a discussion of theoretical Γ_γ values.
- ²⁶F. C. Barker, Aust. J. Phys. 33, 177 (1980); and private communication.
- ²⁷R. G. H. Robertson, P. Dyer, T. J. Bowles, R. E. Brown, N. Jarmie, C. J. Maggiore, and S. M. Austin, Phys. Rev. C 27, 11 (1983).
- ²⁸J. N. Bahcall and R. L. Sears, Annu. Rev. Astron. Astrophys. 10, 25 (1972).